Electronic Supplementary Material (ESI) for Dalton Transactions.

Expanding the Allyl Analogy: Accessing η^3-P,B,P Diphosphinoborane Complexes of Group 10

Marcus W. Drover and Jonas C. Peters*

Division of Chemistry and Chemical Engineering, California Institute of Technology,
Pasadena, California 91125, United States

Figure S1. 1, ^{1}H NMR, C_6D_6, 400 MHz, 298 K

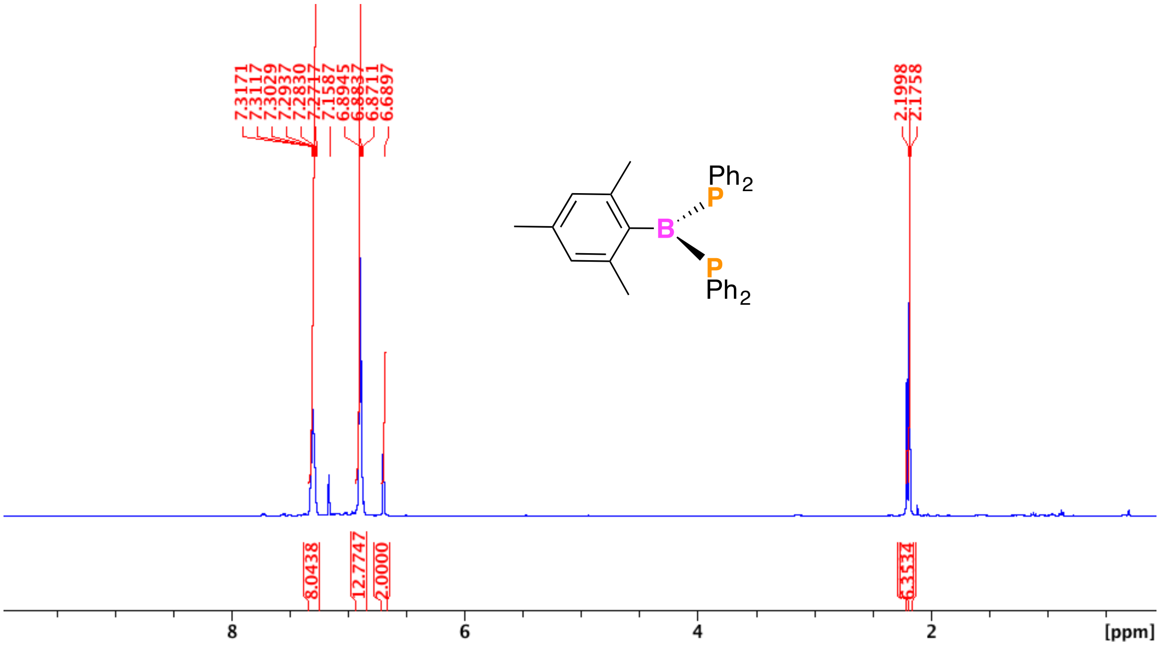

Figure S2. 1, $^{13}C\{^1H\}$ NMR, C_6D_6, 100 MHz, 298 K

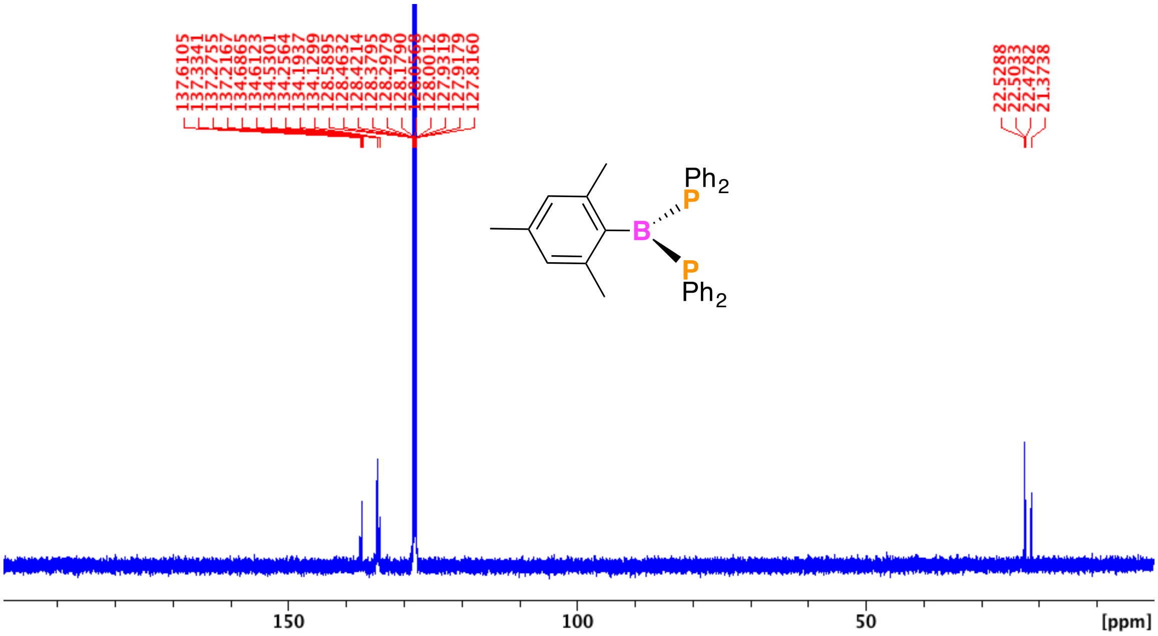

Figure S3. 1, $^{11}B\{^1H\}$ NMR, C_6D_6, 128.3 MHz, 298 K

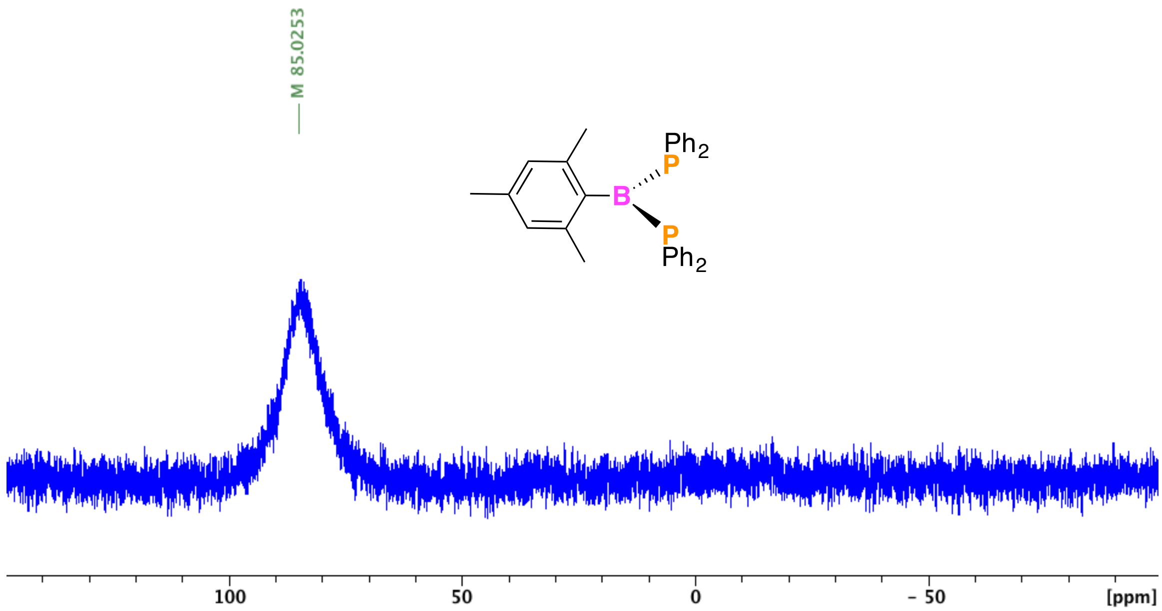

Figure S4. 2, ^1H NMR, THF-d_8, 400 MHz, 298 K (**x** = pentane and Et_2O impurity)

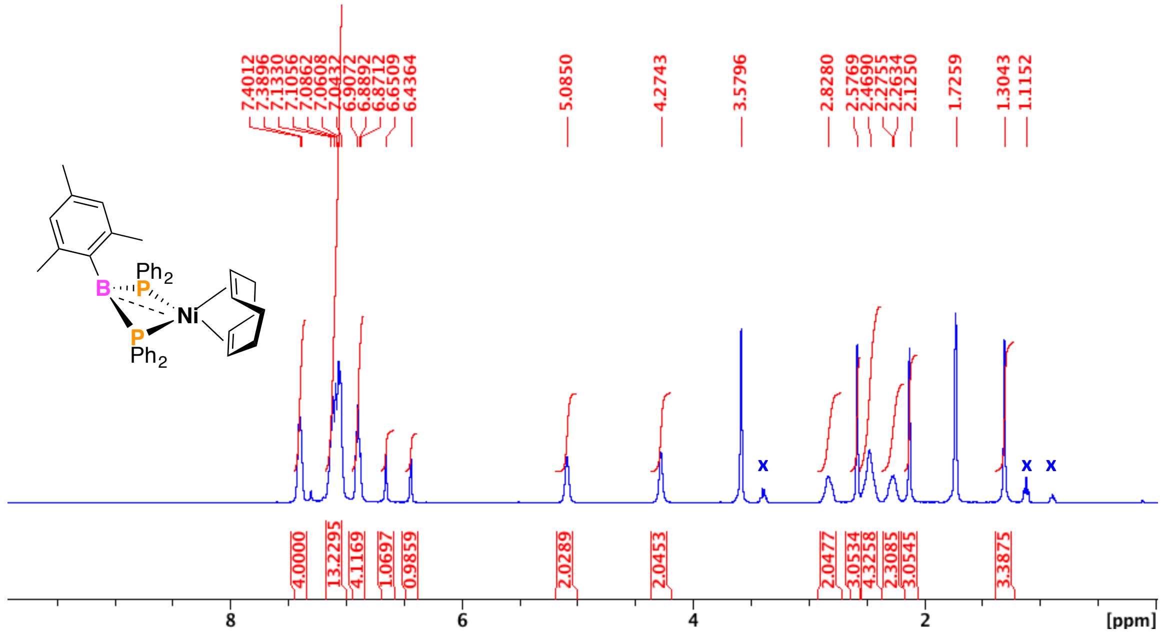

Figure S5. 2, $^{13}C\{^{1}H\}$ NMR, C_6D_6, 100 MHz, 298 K

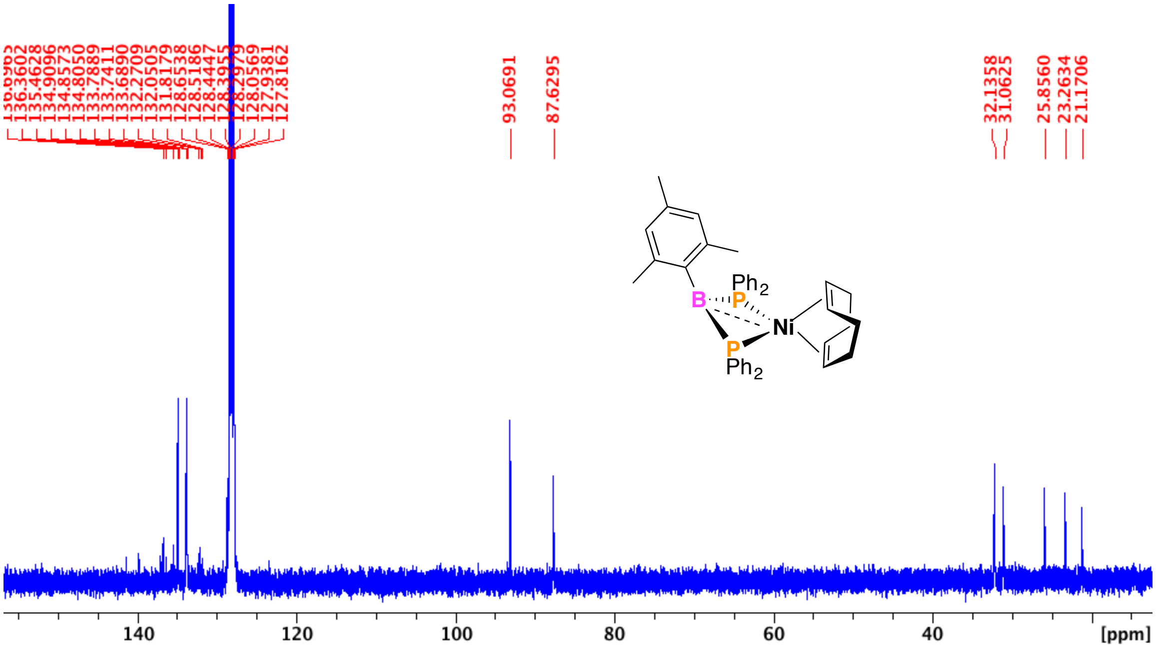

Figure S6. 2, $^{31}P\{^{1}H\}$ NMR, THF-d_8, 161.8 MHz, 298 K

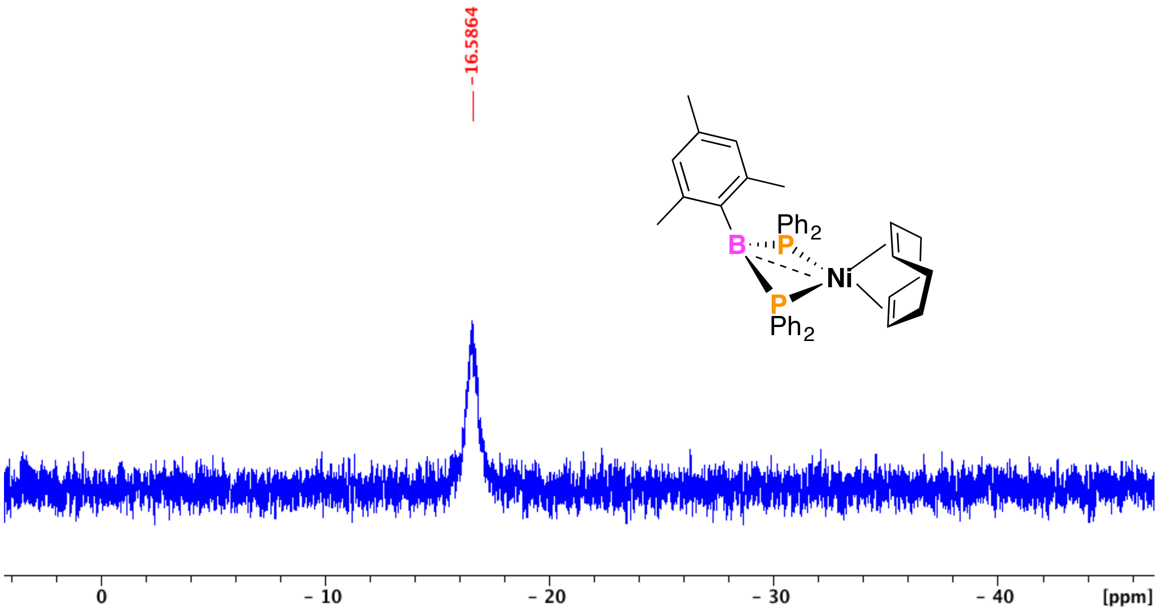

Figure S7. 2, $^{11}B\{^{1}H\}$ NMR, C_6D_6, 128.3 MHz, 298 K

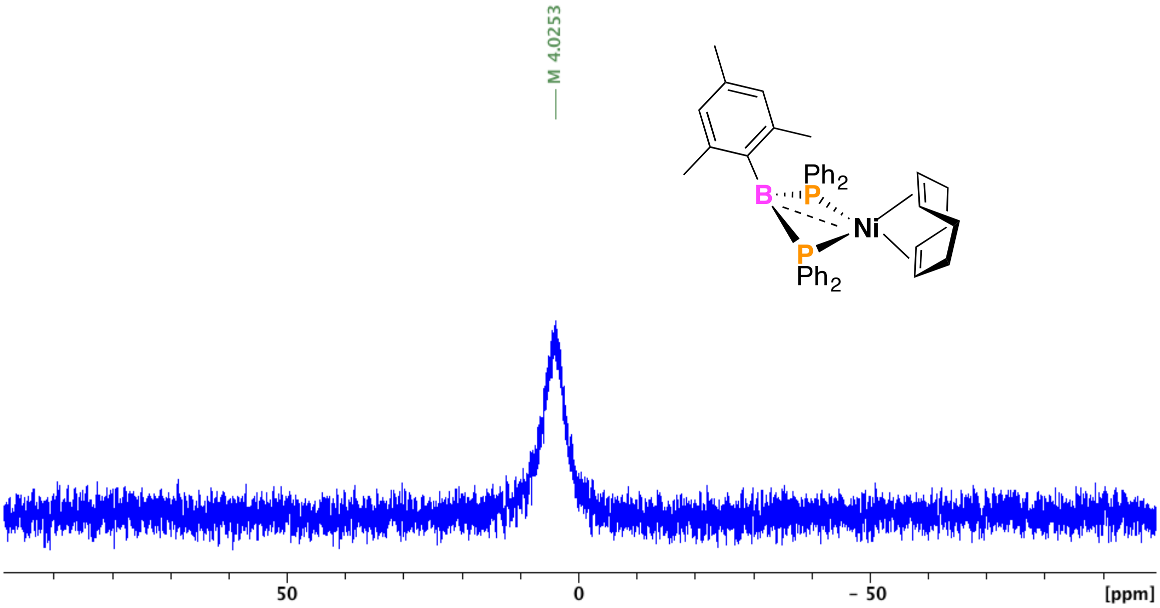

Figure S8. 3, ^{1}H NMR, C_6D_6, 400 MHz, 298 K (**x** = pentane and Et_2O impurity)

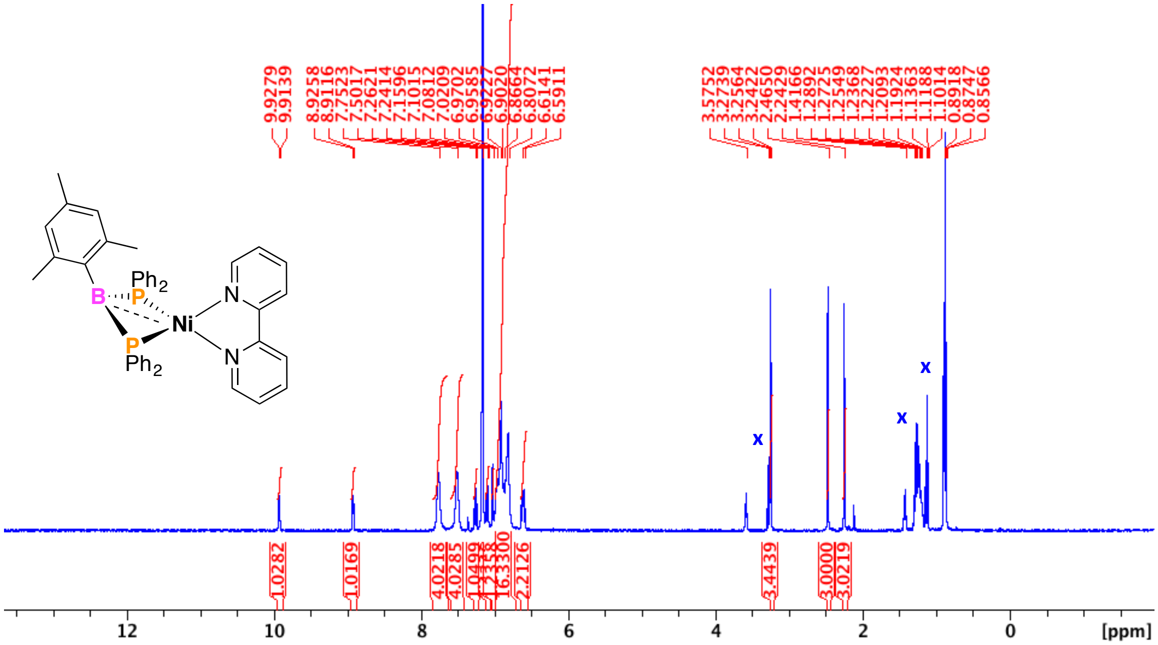

Figure S9. 3, $^{13}C\{^1H\}$ NMR, C_6D_6, 100 MHz, 298 K

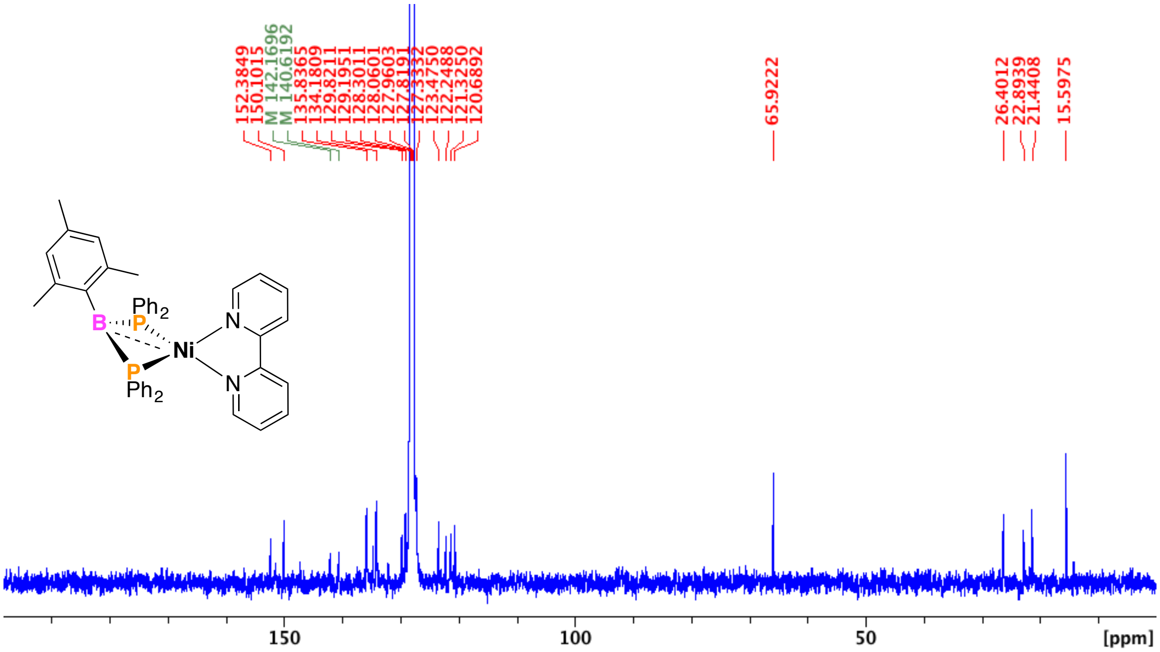

Figure S10. 3, $^{31}P\{^1H\}$ NMR, C_6D_6, 161.8 MHz, 298 K

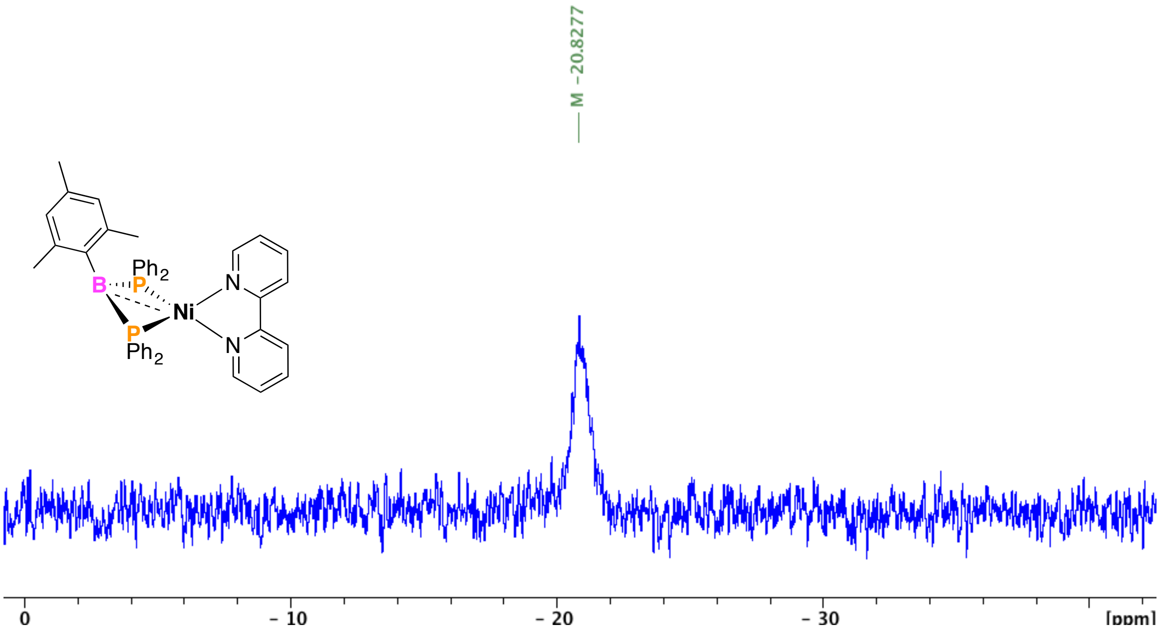

Figure S11. 3, $^{11}B\{^{1}H\}$ NMR, C_6D_6, 128.3 MHz, 298 K

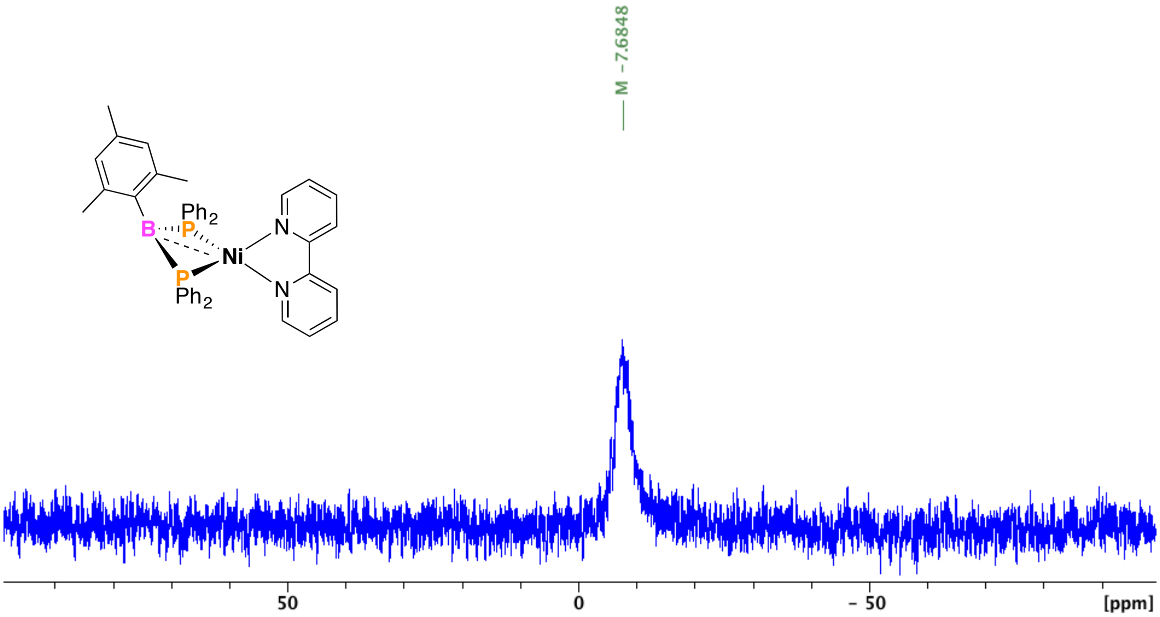

Figure S12. 4, ^{1}H NMR, C_6D_6, 400 MHz, 298 K

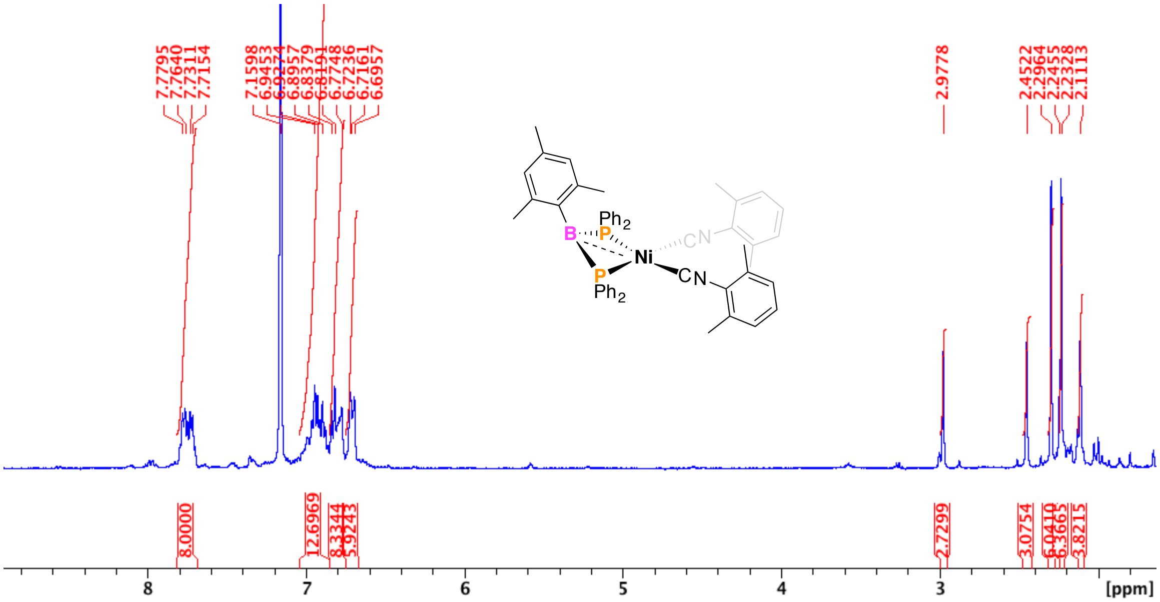

Figure S13. 4, $^{13}C\{^1H\}$ NMR, C_6D_6, 100 MHz, 298 K

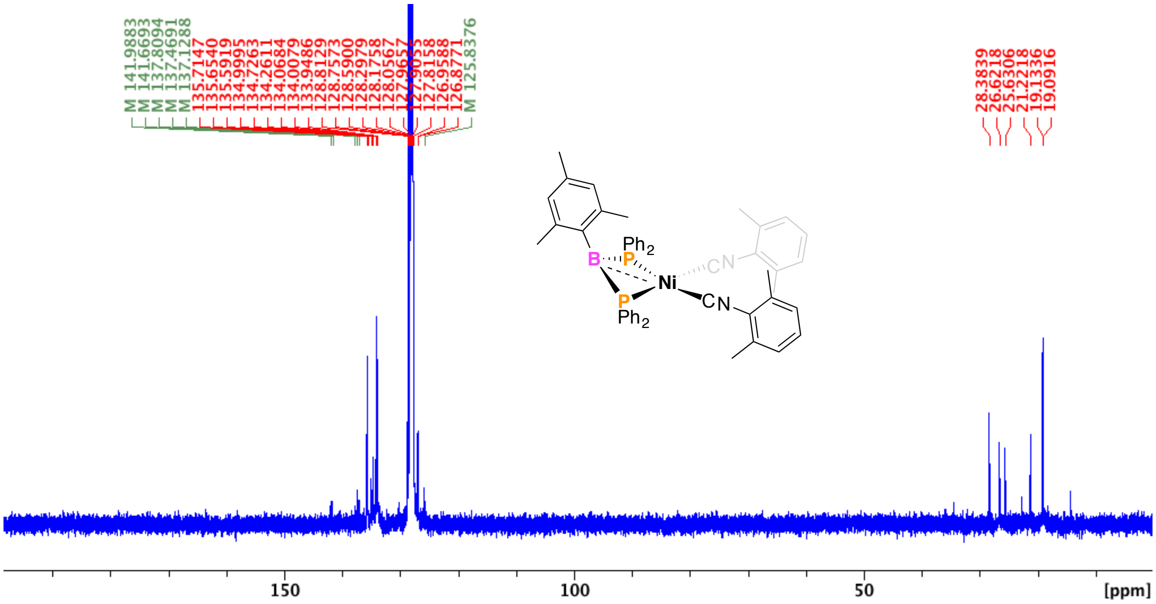

Figure S14. 4, $^{31}P\{^1H\}$ NMR, C_6D_6, 161.8 MHz, 298 K

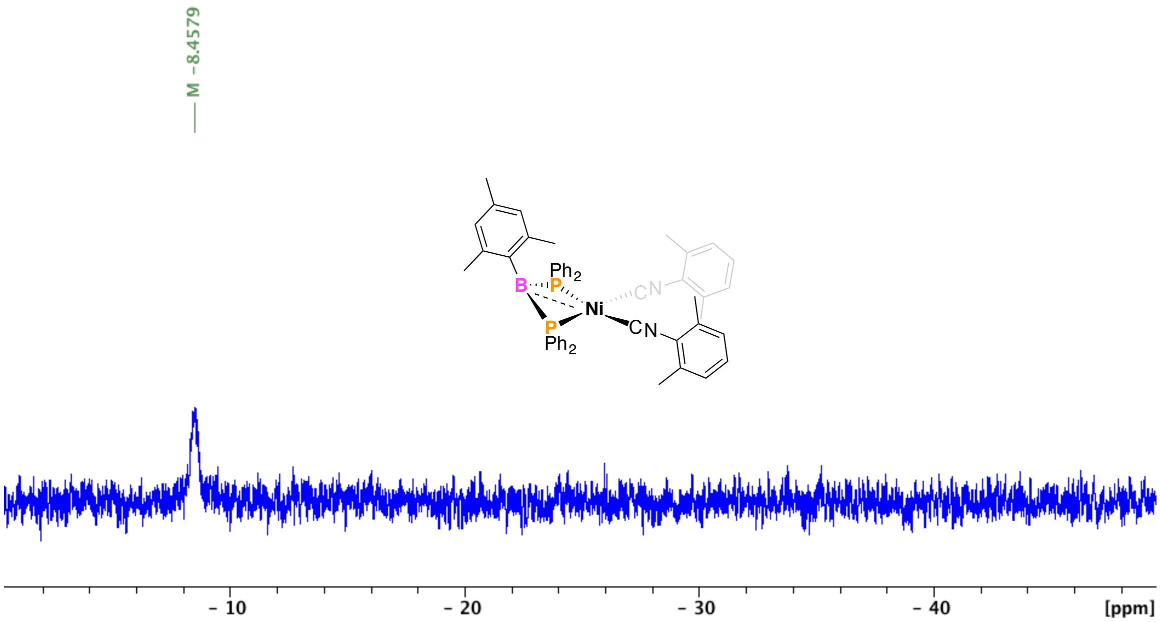

Figure S15. 4, $^{11}B\{^{1}H\}$ NMR, C_6D_6, 128.3 MHz, 298 K (small signal at $\delta_B = 31.2$ ppm is for the boroxin, $(MesBO)_3$)

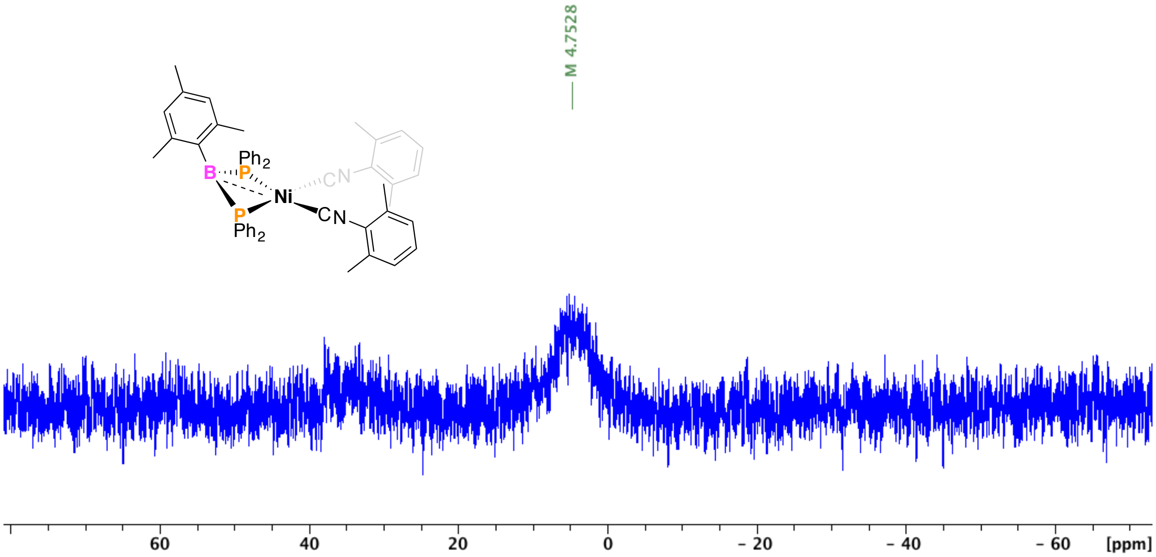

Figure S16. 4, FT-IR ATR, solid film, 298 K

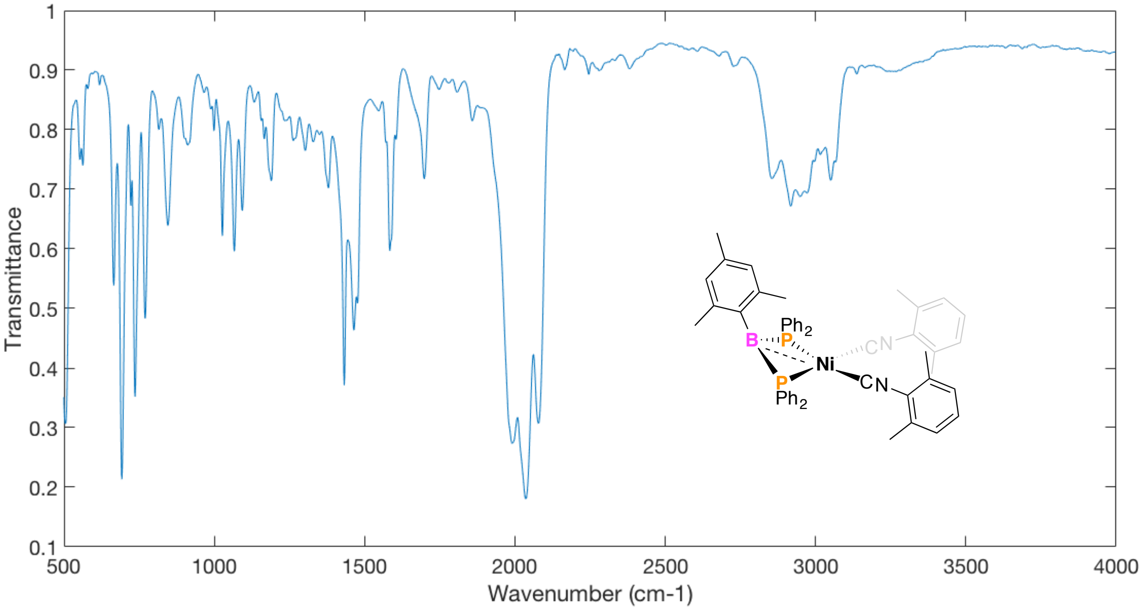

Figure S17. 5, ^{1}H NMR, C_6D_6, 400 MHz, 298 K (**x** = pentane and Et_2O impurity)

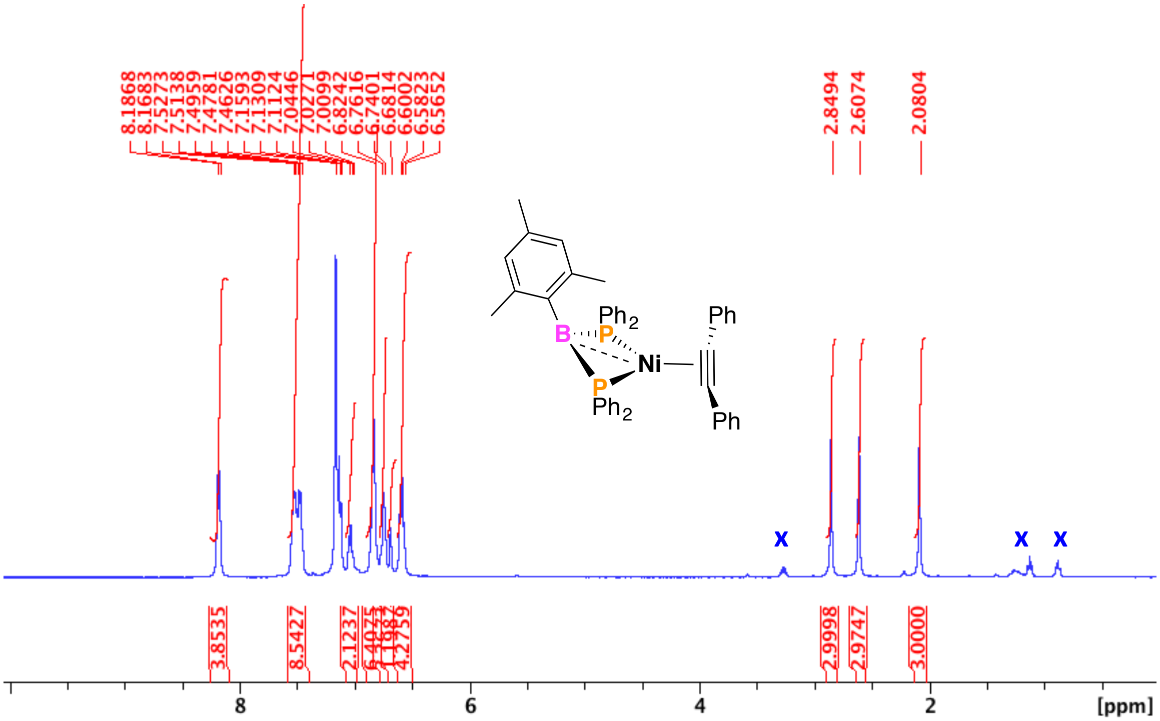

Figure S18. 5, ^{13}C{^{1}H} NMR, C_6D_6, 100 MHz, 298 K

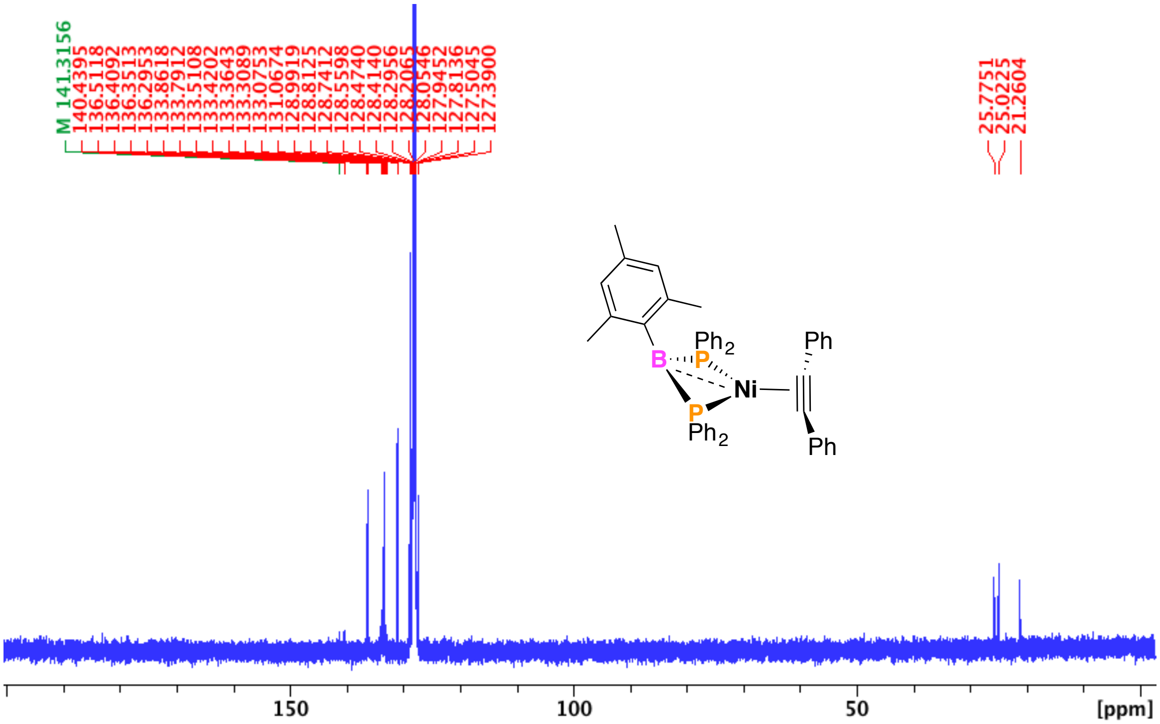

Figure S19. 5, $^{31}P\{^{1}H\}$ NMR, C_6D_6, 161.8 MHz, 298 K

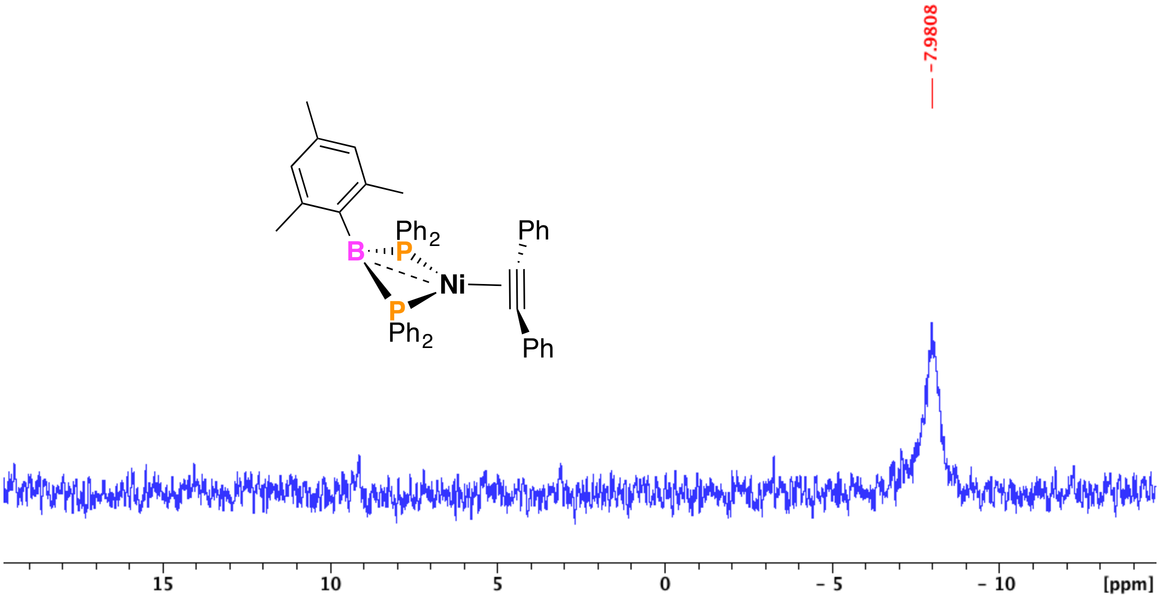

Figure S20. 5, $^{11}B\{^{1}H\}$ NMR, C_6D_6, 128.3 MHz, 298 K

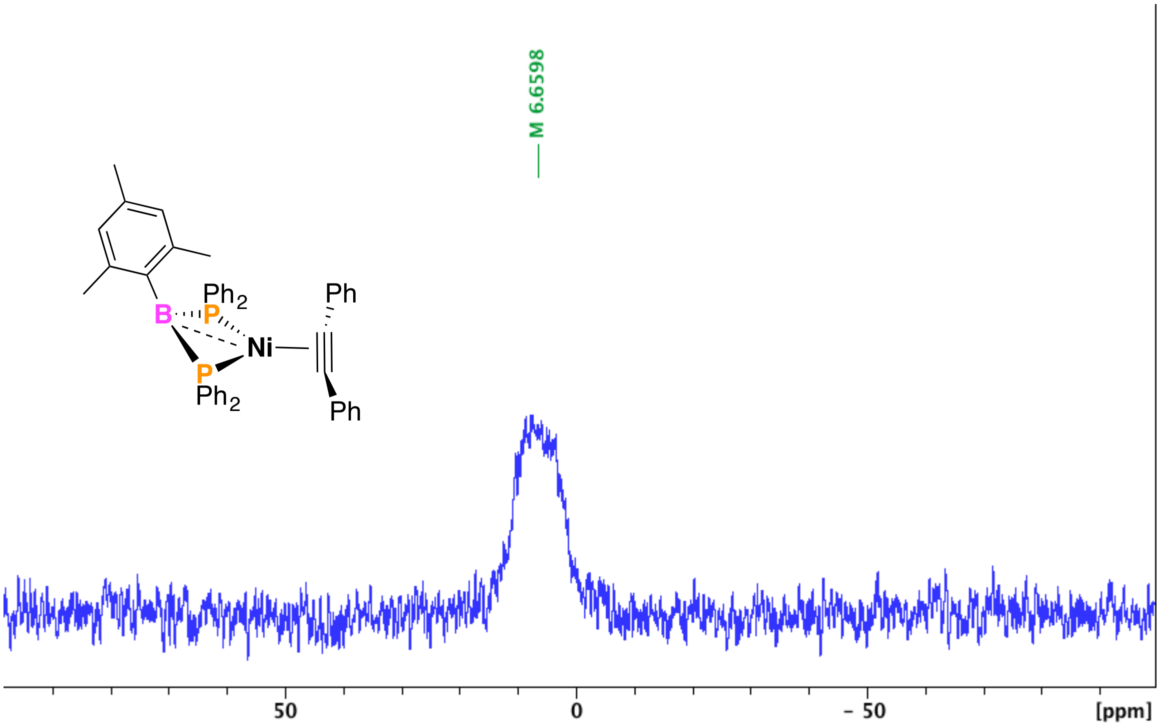

Figure S21. 5, FT-IR ATR, solid film, 298 K

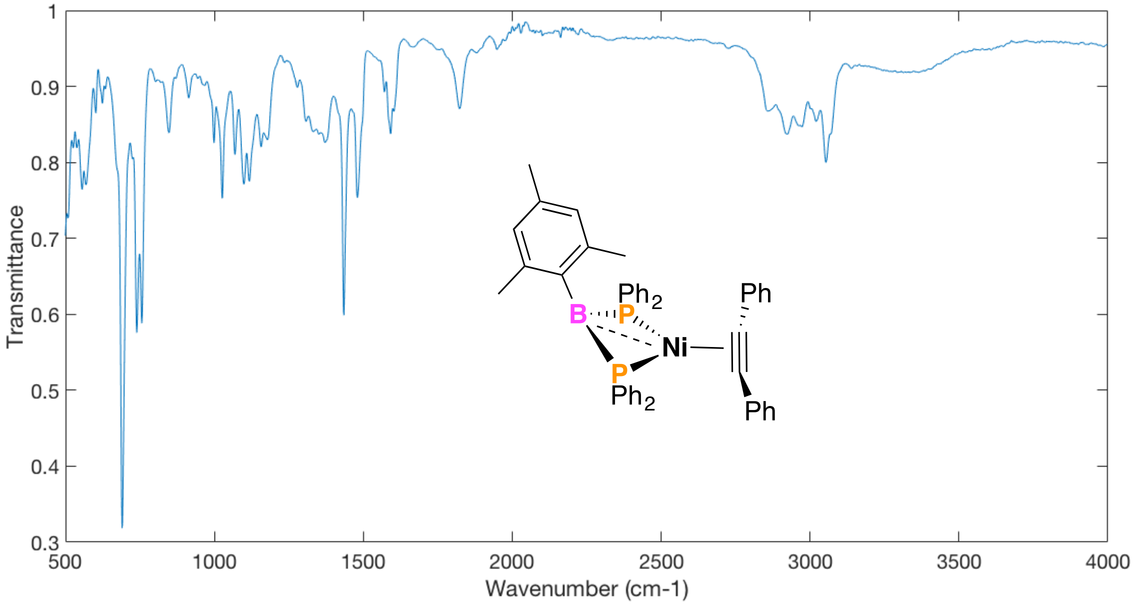

Figure S22. 6, ^{1}H NMR, C_6D_6, 400 MHz, 298 K (inset shows expansion of Pt-C$\underline{H}_3$ signal, **x** = pentane and Et_2O impurity)

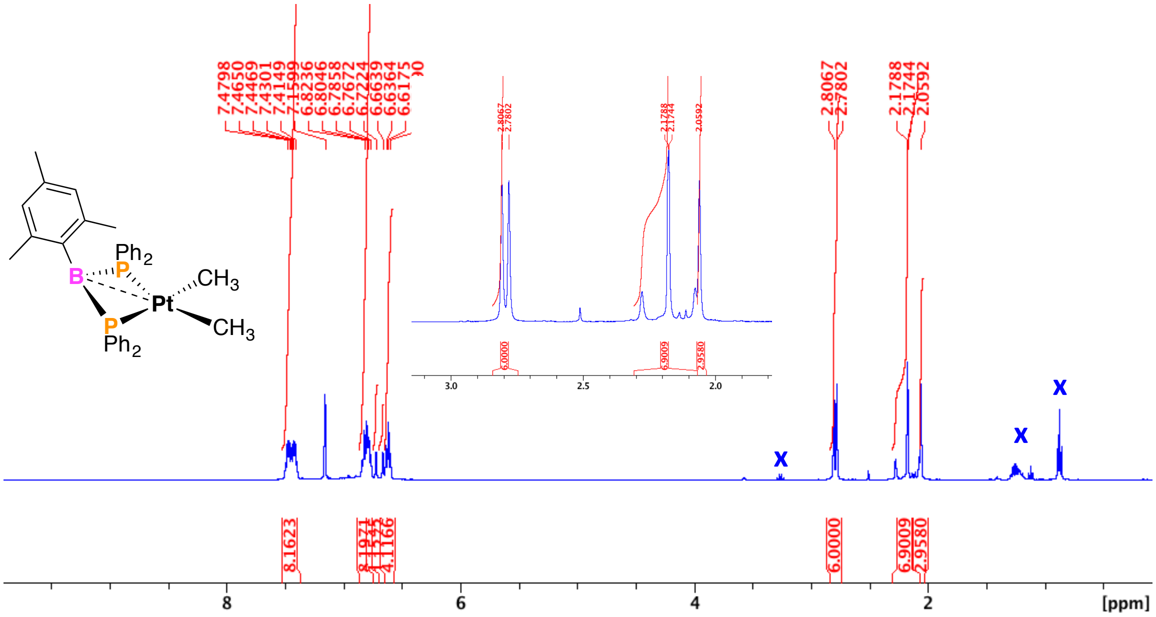

Figure S23. 6, $^{13}C\{^{1}H\}$ NMR, C_6D_6, 100 MHz, 298 K (inset shows expansion of Pt-$\underline{C}H_3$ signal)

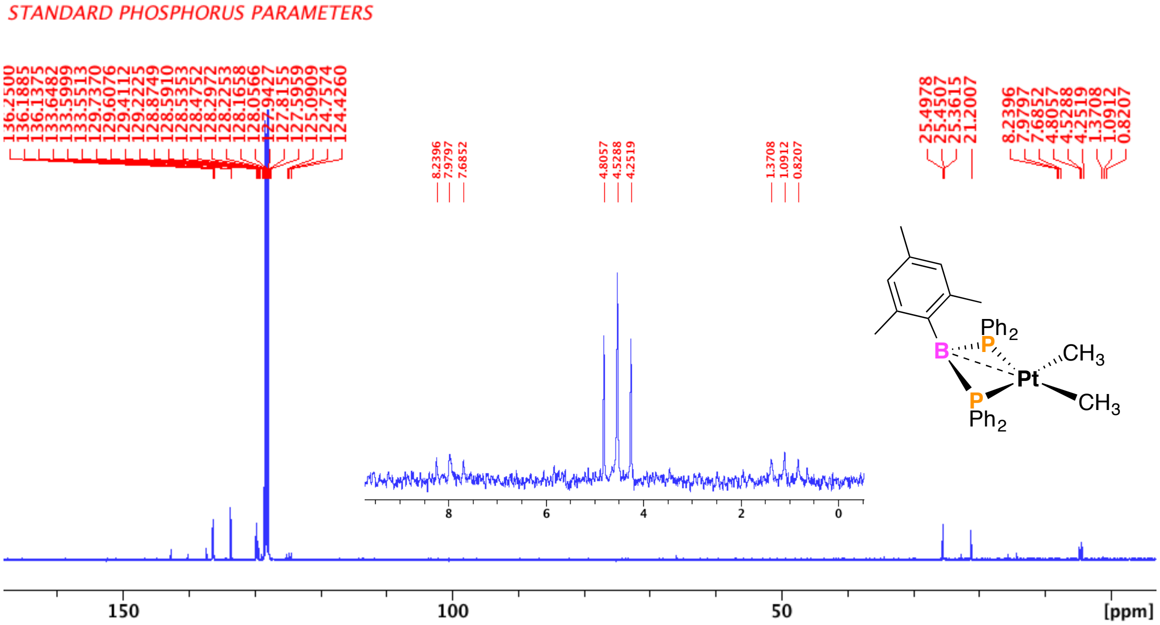

Figure S24. 6, $^{31}P\{^{1}H\}$ NMR, C_6D_6, 161.8 MHz, 298 K

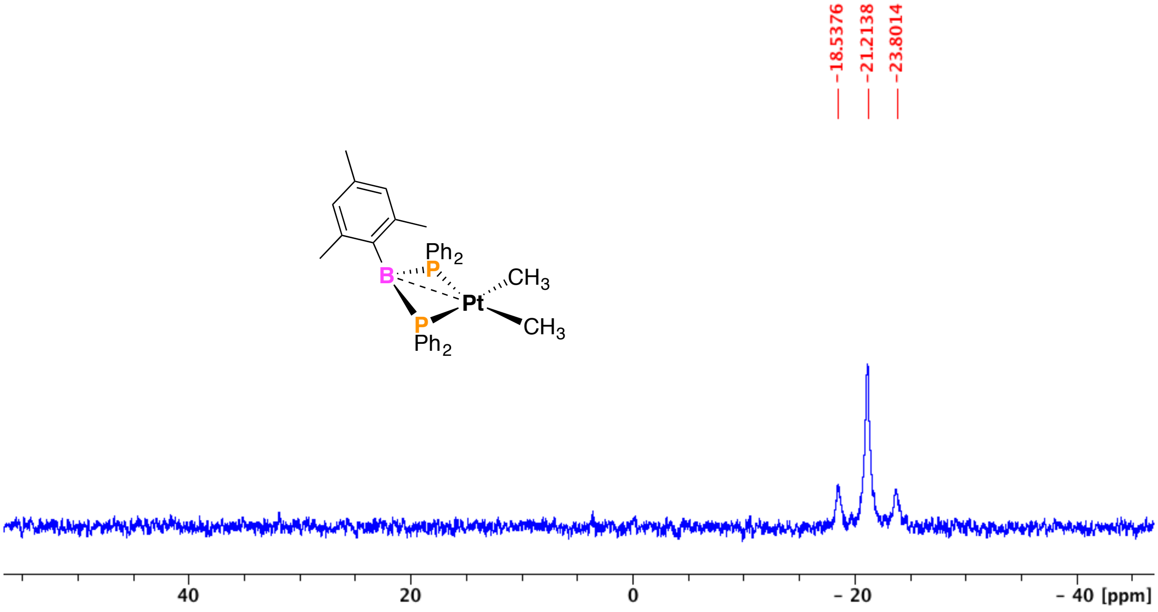

Figure S25. 6, $^{11}B\{^{1}H\}$ NMR, C_6D_6, 128.3 MHz, 298 K (inset shows $^{11}B\{^{1}H\}$ NMR using a quartz tube)

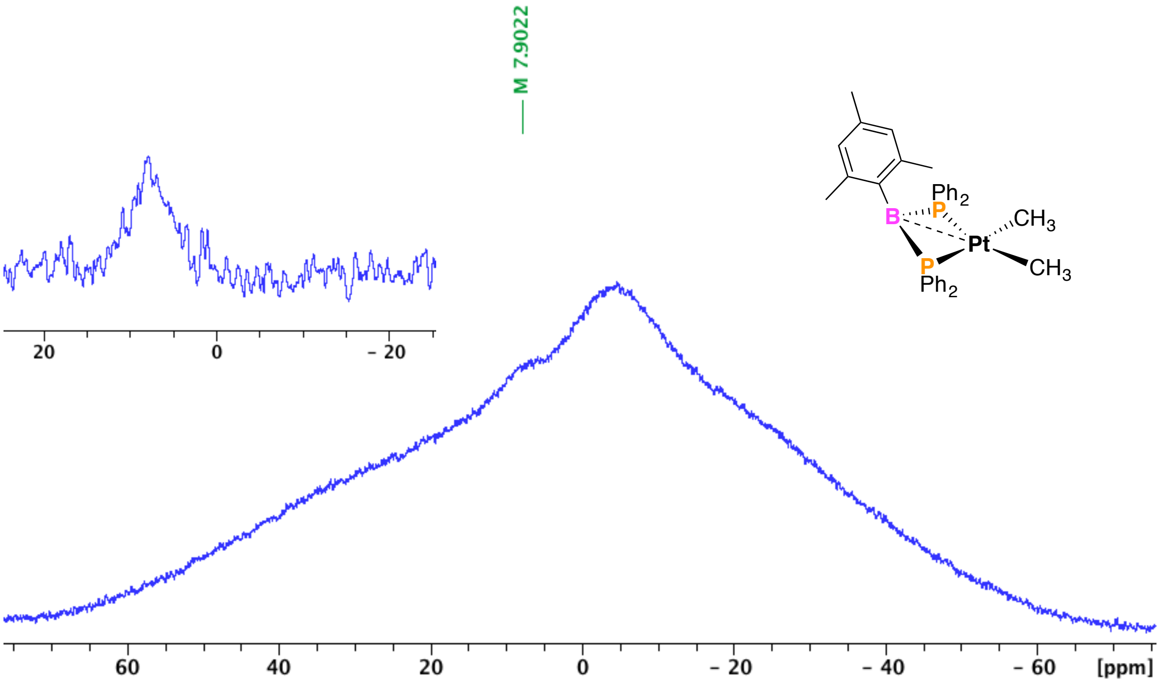

Figure S26. 10, ^{1}H NMR, C_6D_6, 400 MHz, 298 K (**x** = pentane and Et_2O impurity)

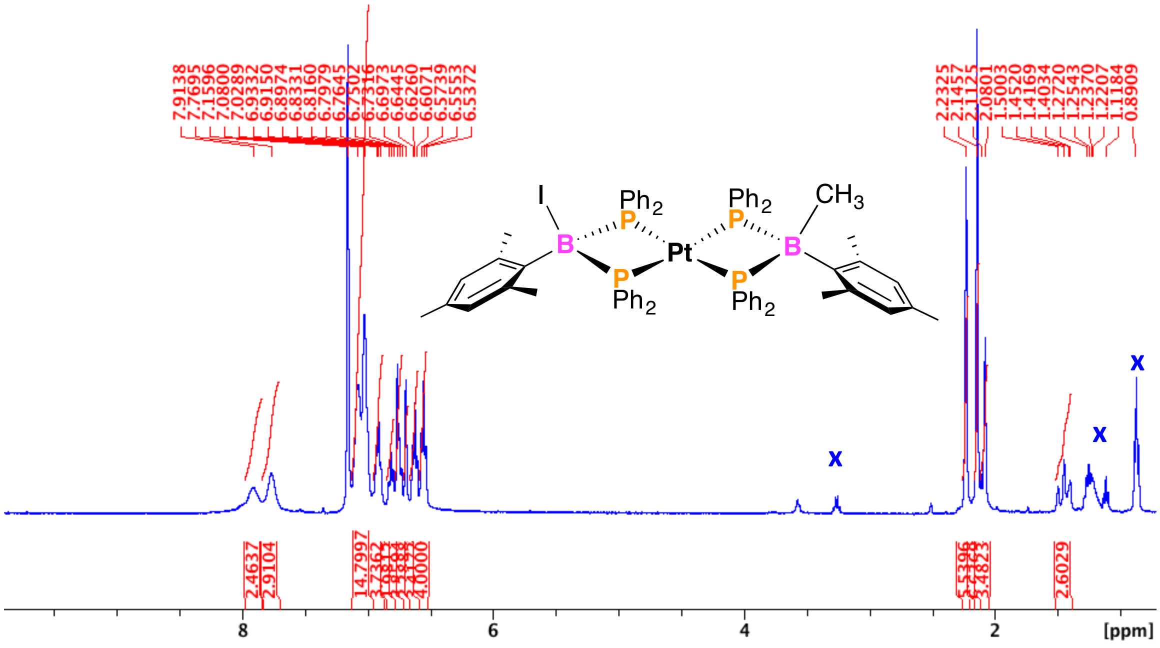

Figure S27. **10**, $^{13}C\{^1H\}$ NMR, THF-d_8, 100 MHz, 298 K

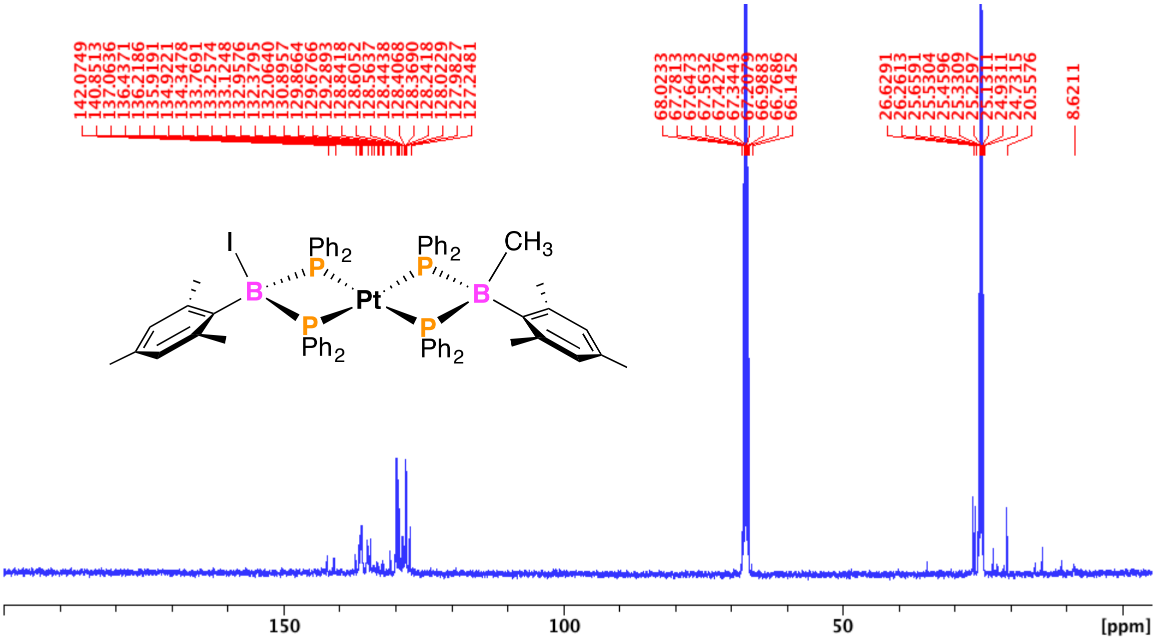

Figure S28. **10**, $^{31}P\{^1H\}$ NMR, C_6D_6, 161.8 MHz, 298 K

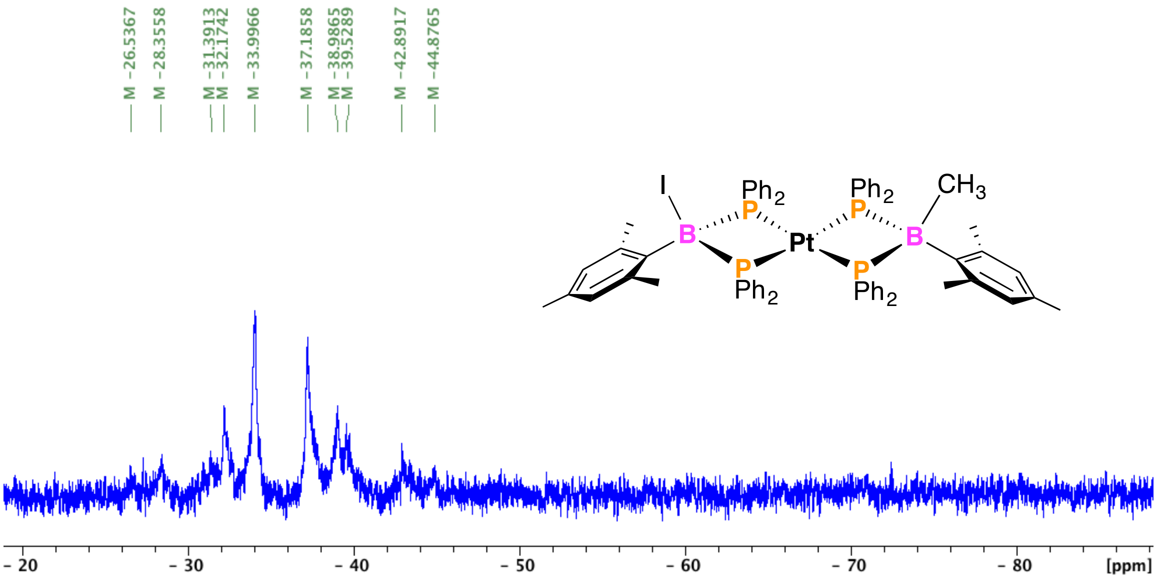

Figure S29. 10, ^{11}B{^{1}H} NMR, C_6D_6, 128.3 MHz, 298 K

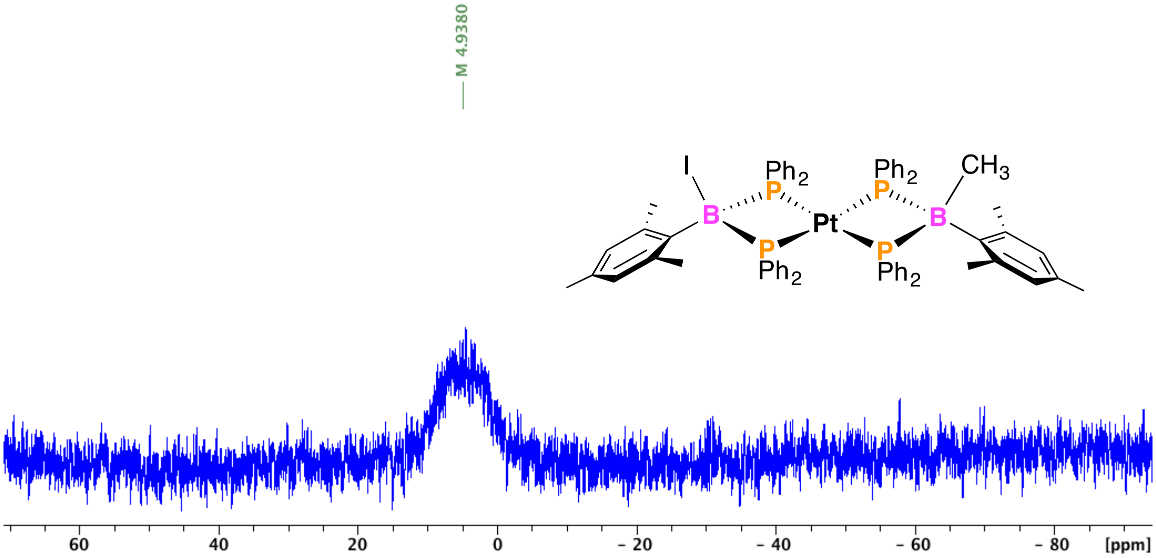

Electrochemical Details:

Cyclic voltammetry (CV) measurements were carried out in a glovebox under an N_2 atmosphere in a one-compartment cell using a CH Instruments 600B electrochemical analyzer. A glassy carbon electrode was used as the working electrode and a carbon rod was used as the auxiliary electrode. The reference electrode was AgOTf/Ag in THF isolated by a CoralPor^{TM} frit (obtained from BASi). The ferrocenium/ferrocene couple (Fc^+/Fc) was used as an external reference. THF solutions of electrolyte (0.2 M $[NBu_4][PF_6]$) and analyte (1 mM) were also prepared under an inert atmosphere.

Figure S30. 2, CV, THF, 298 K showing quasi-reversible wave for the proposed boron-based reduction at *ca.* - 2.65 V.

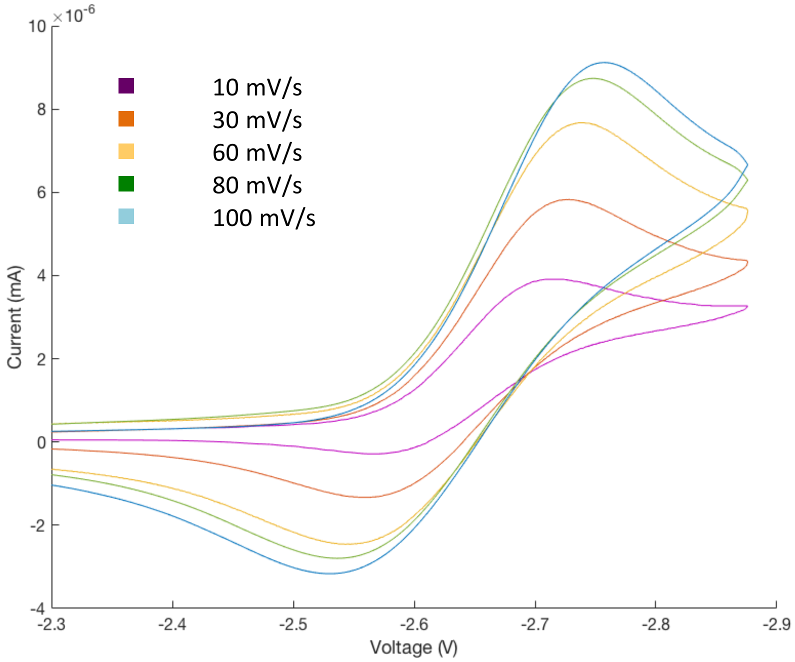

Crystallographic details:

All crystals were mounted on a glass fiber loop. All measurements were made using graphite-monochromated Mo K_α radiation (λ=0.71073 Å) on either a Bruker AXS KAPPA APEX II diffractometer coupled to an APEX II CCD detector (**3**, **6**, and **10**) or a Bruker AXS D8 VENTURE KAPPA diffractometer coupled to a PHOTON 100 CMOS detector (**2** and **5**). The structures were solved by direct methods[3] and refined by full-matrix least-squares procedures on F2 (SHELXL-2013)[3] using the OLEX2 interface.[4] All hydrogen atoms were placed in calculated positions. Non-hydrogen atoms were refined anisotropically.

Additional details:

3: This crystal structure contained residual electron density assignable to two disordered THF molecules. OLEX2 was used to identify voids and a solvent mask was applied [Void volume = 661.8 $Å^3$ corresponding to 160.1 electrons]. This application gave a good improvement of data statistics.

6: A level alerts persist in the *checkcif* file related to 'Calcd Residual Density' close to the heavy Pt center.

10: This crystal structure contained electron density assignable to a disordered pentane molecule about an inversion center. OLEX2 was used to identify voids and a solvent mask was applied [two void volumes = 266.6 $Å^3$ corresponding to 27.8 electrons each]. This application gave a good improvement of data statistics. The B-X groups (X = CH_3 or I) were split over two positions and modeled as a 45/55 split.

$[Pt(HPPh_2)(\mu\text{-}PPh_2)I]_2$: This crystal is a twin. The following twin law was obtained: **TWIN LAW** (-1.0, 0.0, 0.0, 0.0, -1.0, 0.0, 0.0, 0.0, 1.0), **BASF** [0.3219(8)] using OLEX2.

CCDC **1581574-1581579** contains the supplementary crystallographic data for this paper. These data can be obtained free of charge from The Cambridge Crystallographic Data Centre *via* www.ccdc.cam.ac.uk/data_request/cif.

Table S1. Crystallographic data for **2** and **3**:

Compound	**2**	**3**
Empirical formula	$C_{41}H_{43}BNiP_2$	$C_{43}H_{39}BN_2NiP_2$
Formula weight	667.21	715.22
Temperature/K	100(2)	100(2)
Crystal system	Orthorhombic	Triclinic
Space group	$Pna2_1$	$P\text{-}1$
a/Å	16.2090(5)	11.0162(11)
b/Å	12.6755(5)	13.4010(14)
c/Å	16.7152(7)	16.5488(17)
α/°	90	110.291(5)
β/°	90	98.272(6)
γ/°	90	94.867(6)
V/Å^3	3434.3(2)	2243.6(4)
Z	4	2
ρ/ g/cm^{-3}	1.290	1.059
μ/ mm^{-1}	0.687	0.531
F(000)	1408.0	748.0
Crystal size/ mm^3	0.34 × 0.28 × 0.16	0.23 × 0.22 × 0.12
Radiation	MoKα (λ = 0.71073)	MoKα (λ = 0.71073)
2θ range for data collection/°	4.752 to 61.116	3.274 to 59.628
Index ranges	$-22 \leq h \leq 20$, $-17 \leq k \leq 18$, $-23 \leq l \leq 22$	$-15 \leq h \leq 15$, $-18 \leq k \leq 18$, $-22 \leq l \leq 22$
Independent reflections	9731 [R_{int} = 0.0897, R_{sigma} = 0.1185]	12328 [R_{int} = 0.0782, R_{sigma} = 0.0781]
Data/restraints/parameters	9731/430/409	12328/435/445
Goodness-of-fit on F^2	1.011	1.011
R [I>=2θ (I)] (R1, wR2)	$R_1 = 0.0532$, $wR_2 = 0.0722$	$R_1 = 0.0658$, $wR_2 = 0.1757$
R (all data) (R1, wR2)	$R_1 = 0.1009$, $wR_2 = 0.0816$	$R_1 = 0.0868$, $wR_2 = 0.1902$
Largest diff. peak/hole / (e Å^{-3})	0.67/-0.42	2.02/-1.36
Flack parameter	0.009(8)	--

$R1 = \Sigma \, ||F_o|-|F_c|| \, / \, \Sigma \, |F_o|$; $wR2 = [\Sigma(w(F_o^2 - F_c^2)^2) \, / \, \Sigma \, w(F_o^2)^2]^{1/2}$

Table S2. Crystallographic data for **5** and **6**:

Compound	**5**	**6**
Empirical formula	$C_{52}H_{53}BNiP_2$	$C_{35}H_{37}BP_2Pt$
Formula weight	809.40	725.48
Temperature/K	100(2)	100(2)
Crystal system	Triclinic	Triclinic
Space group	*P-1*	*P-1*
a/Å	12.1658(7)	10.4431(11)
b/Å	13.5588(9)	12.0491(12)
c/Å	14.0817(9)	13.1755(12)
α/°	77.118(2)	96.138(7)
β/°	70.587(2)	109.587(7)
γ/°	85.824(2)	100.699(7)
V/Å^3	2135.6(2)	1508.9(3)
Z	2	2
ρ/ g/cm^{-3}	1.259	1.597
μ/ mm^{-1}	0.564	4.778
F(000)	856.0	720.0
Crystal size/ mm^3	0.27 × 0.16 × 0.16	0.25 × 0.19 × 0.08
Radiation	MoKα (λ = 0.71073)	MoKα (λ = 0.71073)
2θ range for data collection/°	4.698 to 58.302	3.338 to 55.576
Index ranges	$-16 \le h \le 16$, $-18 \le k \le 18$, $-19 \le l \le 19$	$-13 \le h \le 13$, $-15 \le k \le 15$, $-17 \le l \le 17$
Independent reflections	11513 [R_{int} = 0.0914, R_{sigma} = 0.0610]	6510 [R_{int} = 0.0791, R_{sigma} = 0.0899]
Data/restraints/parameters	11513/0/510	6510/336/357
Goodness-of-fit on F^2	1.046	1.051
R [I>=2θ (I)] (R1, wR2)	$R_1 = 0.0575$, $wR_2 = 0.1215$	$R_1 = 0.0567$, $wR_2 = 0.1341$
R (all data) (R1, wR2)	$R_1 = 0.0922$, $wR_2 = 0.1348$	$R_1 = 0.0845$, $wR_2 = 0.1487$
Largest diff. peak/hole / (e Å^{-3})	1.46/-1.18	4.24/-1.86

$R1 = \Sigma ||F_o|-|F_c|| / \Sigma |F_o|$; $wR2 = [\Sigma(w(F_o^2 - F_c^2)^2) / \Sigma w(F_o^2)^2]^{1/2}$

Table S3. Crystallographic data for **10** and **[Pt(HPPh$_2$)(μ-PPh$_2$)I]$_2$**:

Compound	**10**	**[Pt(HPPh$_2$)(μ-PPh$_2$)I]$_2$**
Empirical formula	$C_{70.88}H_{74.65}B_2I_{1.12}OP_4Pt$	$C_{48}H_{42}I_2P_4Pt_2$
Formula weight	1424.94	1386.67
Temperature/K	100(2)	100(2)
Crystal system	Monoclinic	Monoclinic
Space group	*P2$_1$/n*	*P2$_1$/n*
a/Å	12.3295(6)	10.4494(6)
b/Å	19.2099(9)	9.2354(5)
c/Å	27.5709(13)	23.1562(13)
α/°	90	90
β/°	94.522(2)	90.078(2)
γ/°	90	90
V/Å^3	6509.8(5)	2234.7(2)
Z	4	2
ρ/ g/cm^{-3}	1.454	2.061
μ/ mm^{-1}	2.826	7.811
F(000)	2861.0	1304.0
Crystal size/ mm^3	0.2 × 0.16 × 0.12	0.22 × 0.18 × 0.12
Radiation	MoKα (λ = 0.71073)	MoKα (λ = 0.71073)
2θ range for data collection/°	2.964 to 60.128	4.274 to 61.014
Index ranges	$-16 \le h \le 16$, $-26 \le k \le 26$, $-37 \le l \le 37$	$-14 \le h \le 14$, $-13 \le k \le 13$, $-33 \le l \le 32$
Independent reflections	17777 [R_{int} = 0.0766, R_{sigma} = 0.0392]	6818 [R_{int} = 0.0689, R_{sigma} = 0.0572]
Data/restraints/parameters	17777/6/750	6818/0/254
Goodness-of-fit on *F*^{2}	1.072	1.089
R [I>=2θ (I)] (R1, wR2)	R_1 = 0.0334, wR_2 = 0.0722	R_1 = 0.0350, wR_2 = 0.0698
R (all data) (R1, wR2)	R_1 = 0.0486, wR_2 = 0.0757	R_1 = 0.0467, wR_2 = 0.0804
Largest diff. peak/hole / (e Å^{-3})	2.48/-1.19	1.34/-1.58

$R1 = \Sigma ||F_o|-|F_c|| / \Sigma |F_o|$; $wR2 = [\Sigma(w(F_o^2 - F_c^2)^2) / \Sigma w(F_o^2)^2]^{1/2}$

Figure S31. ORTEP depiction of the solid-state molecular structure of **[Pt(HPPh$_2$)(μ-PPh$_2$)I]$_2$** isolated as an impurity from reaction of ligand **1** and 0.25 equiv. of [Pt(CH$_3$)$_3$I]$_4$ (displacement ellipsoids are shown at the 50% probability). Selected bond lengths [Å]: Pt(1)-I(1) 2.6567(5), Pt(1)-P(1) 2.306(2), Pt(1)-P(2) 2.326(2).

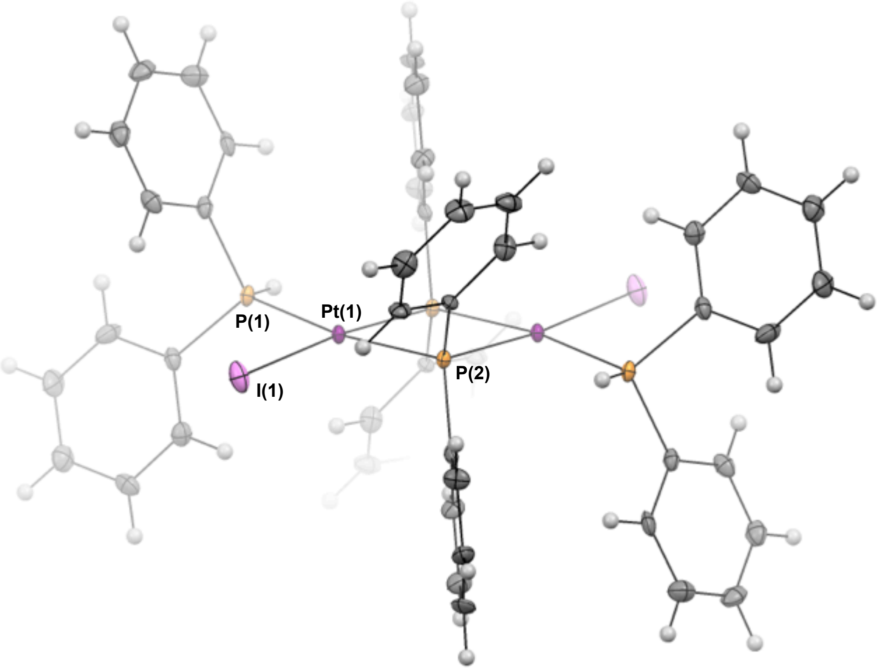

References:

1 R. A. Bartlett, H. Dias and P. P. Power, *Inorg. Chem.*, 1988, **27**, 3919–3922.

2 S. C. Cole, M. P. Coles and P. B. Hitchcock, *Dalton Trans.*, 2003, 3663.

3 G. M. Sheldrick, *Acta Crystallogr., Sect. A: Found. Crystallogr.*, 2008, **64**, 112–122.

4 O. V. Dolomanov, L. J. Bourhis, R. J. Gildea, J. A. K. Howard and H. Puschmann, *J. Appl. Crystallogr.*, 2009, **42**, 339–341.